Desalination and Water Treatment
www.deswater.com

doi: 10.5004/dwt.2021.26741

214 (2021) 413–419
February

Contribution of photocatalysis for the elimination of Methyl Orange (MO) in aqueous medium using TiO_2 catalyst, optimization of the parameters and kinetics modeling

Moussa Abbas[a,*], Mohamed Trari[b]

[a]*Laboratory of Soft Technologies, Valorization, Physicochemistry of Biological Materials and Biodiversity (LTDVPMBB), Faculty of Sciences, University M'hamed Bougara, Boumerdes 35000, Algeria, Tel. +213 552408419; Fax: +213 21 24 80 08; emails: moussaiap@gmail.com/m.abbas@univ-boumerdes.dz*
[b]*Laboratory of Storage and Valorization of Renewable Energies, Faculty of Chemistry (USTHB), BP 32-16111 Algiers, Algeria, emails: solarchemistry@gmail.com/mtrari@usthb.dz*

Received 16 February 2020; Accepted 25 October 2020

ABSTRACT

The photo degradation of methyl orange (MO) in water onto TiO_2 under UV irradiation is investigated. The parameters (MO concentration, catalyst dose, time, flux intensity and pH) influencing the degradation kinetics are studied. The equilibrium adsorption time of MO in the presence of TiO_2 is reached after 50 min of contact. Addition of H_2O_2 and NaCl at concentrations ranging from 100 to 500 ppm shows that the percentage of the photo degradation decreases with increasing the H_2O_2 concentration. The best results are obtained for a concentration of 100 mg/L, while NaCl has a negative effect on the MO photo degradation. The photocatalytic degradation rate was favored at high MO concentrations in agreement with the Langmuir–Hinshelwood (L-H) model. The constants k_r and K for the MO photo degradation are found to be 0.048 mg L/min and 16.246 L/mg, respectively.

Keywords: Photocatalysis; Pollutant; TiO_2; Methyl Orange; UV irradiation; Modeling

---

1. Introduction

Photo catalysts have received enormous attention as effective and sustainable materials for the removal of inorganic, organic (dyes, pesticides) and carcinogenic pollutants from water, which causes hazardous effects on the human health and environment and must be converted into harmless species as CO_2, H_2O, etc. [1]. These nano structured materials have excellent physical and chemical properties making them suitable for applications in nano devices [2]. TiO_2, In_2O_3, NiO, SnO_2 and ZnO are among the most popular semiconductors, which attracted a great attention due to their chemical stability, low toxicity and especially their high photo degradation ability [2]. When a photocatalyst is exposed to UV/visible light, electrons (e^-) gain energy and get transferred to the conduction band leaving CB a hole (h^+) in the valence band thus VB producing (e^- – h^+) pairs (excitons). TiO_2 is a vital nanomaterial, which has attracted an impressive consideration due to its new properties. TiO_2 has great merits in the solar conversion and photocatalysis of toxic substances in the environmental conditions. The inactivity of the preparation and the nontoxic quality of TiO_2 also made it a predominant photocatalyst [3–5]. It has a large band gap (E_g ~ 3.2 eV) and only a small part of sunlight can be absorbed [6]. However, the wide gap permits to generate reactive radicals $^{\bullet}OH$ and $O_2^{\bullet-}$ responsible for the mineralization of the organic pollutants.

Water pollution due to the release of various toxic chemicals from industrialization and urbanization is a global problem and a serious threat for the air, soil and water [7]. Among the various notorious toxic chemicals, dyes, organics

---

* Corresponding author.

and pharmaceuticals are very concerned. However, industrial effluents released from the textile, paint, paper, varnish, pulp, cosmetics, tannery and plastic are among the main causes of the water pollution, as these runoffs comprise highly colored substances. Their discharge into the hydrosphere is one of the main sources of pollution due to their reduced visibility even at low concentrations. This is due to their recalcitrant nature, giving undesirable color to the water, reducing sunlight penetration and resistance to both photochemical and biological attacks; their degradation products are toxic or even mutagenic and carcinogenic. There are many studies carried out on the techniques for the removal of dyes including adsorption [8–12], photochemical and biological degradations, coagulation, chemical oxidation, reverse osmosis, flotation and adsorption. The azo dyes (anionic) with the existence of nitrogen–nitrogen double bonds are considered to be the largest and most versatile class of organic dyes [13]. Therefore, their degradation is difficult due to their complicated aromatic and mesomeric structures and poor biodegradability. Methyl orange (MO) is a typical water-soluble anionic azo dye whose IUPAC name is sodium 4-[[4-(dimethyl amino) phenyl] diazenyl] benzene sulfonate. MO is commonly present in the effluents from textile, food, pharmaceutical, printing and paper manufacturing industries [14]. Due to its toxicity and persistence, its discharge can cause a serious threat to the aquatic life. Therefore, it is necessary to find suitable technologies for its elimination from the environment. Therefore, the main objective of the present work is to investigate the potential of TiO_2 as photocatalyst for the MO degradation from aqueous solutions. The effects of the pH, initial MO concentration, contact time, and TiO_2 dosage that influence the degradation processes of MO onto TiO_2 are evaluated.

2. Materials and methods

2.1. Materials

Methyl orange (MO) was supplied by Sigma Chemicals company (Tunisia), and used as adsorbate in the adsorption and photocatalytic tests. Its chemical structure is shown in Fig. 1 and the physical and chemical properties are summarized in Table 1. The MO concentrations were analyzed with a UV-vis spectrophotometer at the maximum wavelength (λ_{max} = 464 nm). The studied parameters for the optimization are TiO_2 dosage (0.5–1.5 g/L), pH (2.5–10), MO concentration (10–30 mg/L) and contact time (0–250 min), while the temperature was maintained constant at 25°C. The photo-reactor consists of a Pyrex beaker (capacity 250 mL), placed in a bath thermostatically controlled at 25°C. Non-plunging UV radiation comes from a 130 W mercury vapor bulb, placed in a stainless steel cooling tube; the suspension was agitated by a magnetic stirrer. Dissolved oxygen was transferred from the air through the surface of the reactor. The photo degradation experiments were performed in a temperature-controlled water bath shaker at 200 rpm. The supernatant was titrated using a UV-vis spectrophotometer at 464 nm for the determination of the residual MO concentration. The photocatalyst used in this study was a commercial TiO_2 purchased from Ahlstrom firm, which consists of PC500 Titania by Millennium Inorganic Chemicals (Chemical Plant in Chaignes, 12 Chemin Du Val Du Puits, 27120 Chaignes, France) (anatase > 99%), a specific surface area (350–400 m^2/g) and a mean crystallite size (5–10 nm). The pH of the solution greatly affects the surface charge of TiO_2 and the size of the aggregates; the pH for which the surface charge of the oxide is zero (point of zero charge: pH_{PZC}) is around 6.5. Before and after this pH, the surface of the oxide is charged positively and negatively:

Table 1
Physicochemical properties of methyl orange

Property	Value
Chemical formula	$C_{14}H_{14}N_3NaO_3S$
Molar mass	327.33 g/mol
Solubility in water	5.20 g/L at 20°C
pKa	3.39
Abbreviation	MO
C.I.	Acid orange 52 Orange III
N° CE	p-Dimethylamino-azobenzene sulfonic acid 208–925–3
The free ph of methyl orange is	6.5

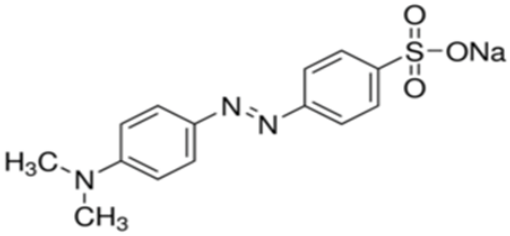

Fig. 1. Structure of Methyl Orange.

$$TiOH_2^+ \longrightarrow TiOH + H^+ \qquad pH < 6.5 \qquad (A)$$

$$TiOH \longrightarrow TiO^- + H^+ \qquad pH > 6.5 \qquad (B)$$

Under these conditions, the photocatalytic degradation of ionized organic compounds will be affected by the pH resulting in repulsive interactions between the ionized pollutant and the surface charge of the photocatalyst, thus reducing the probability of encountering the photocatalyst.

2.2. Spectrophotometric characteristics of methyl orange

Fig. 2 shows the UV-visible adsorption spectrum of MO in aqueous solution; we can determine the maximum wavelength to perform the assay, that is, the wavelength for which the dye MO has a maximum absorption (λ = 465 nm). The synthesis reaction of MO can be broken down schematically into two main stages:

A first step in which the primary amine is transformed into a diazonium ion by the action of nitrous acid. The latter being particularly unstable and sodium nitrite (Na^+, NO_2^-) is in fact used in acid medium:

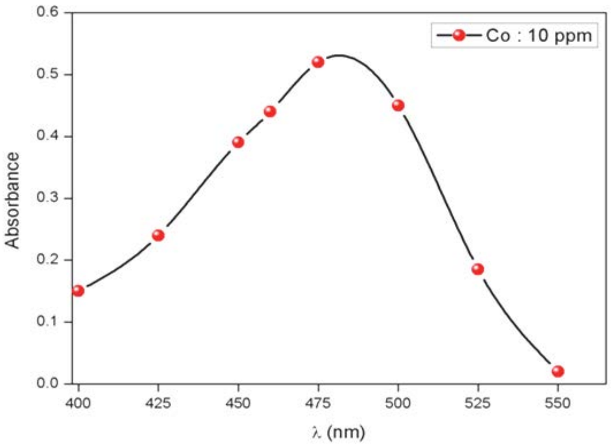

Fig. 2. Visible adsorption spectrum of methyl orange in aqueous solution.

$$O{=}N{-}OH + N{-}RH_2 + H^+ \longrightarrow R{-}N^+ \equiv N + 2\,H_2O \qquad (C)$$

The second step leads the substituted diazonium cation to react with a benzene derivative by aromatic electrophilic substitution:

$$R{-}N^+ \equiv N + H{-}R' \longrightarrow R{-}N{=}N{-}R' + H^+ \qquad (D)$$

In our case, we choose R = HO_3S–Ph and R′ = Ph–N$(CH_3)_2$ to form helianthine.

2.3. Adsorption equilibrium study

The pollutant adsorption on the surface of the catalyst is the initial step and essential for the photocatalysis, where the heterogeneous process requires contact between the molecule MO and the catalyst. Therefore, the interaction between the solid photocatalyst and the organic molecule in the aqueous phase plays an important role in the mechanism of the photocatalytic degradation. Fig. 3 shows that after 50 min, the concentration is almost stabilized (24 mg/L) inside the reactor. To ensure that the equilibrium state is effectively reached, the solution is left in contact with the catalyst in the dark for 70 min. The kinetic laws in such reactions seldom follow proper models and hence are inherently more difficult to formulate from the data. It has been widely accepted that the heterogeneous catalytic reactions can be analyzed with the help of the Langmuir Hinshelwood (L-H) Model [15], with the following assumptions being satisfied:

- There is limited number of adsorption sites on the homogeneous catalyst surface. Only one molecule can be adsorbed on one site and a monolayer formation occurs.
- The absorption reaction is reversible in nature.
- The adsorbed molecules do not react with each other [16].

According to L-H Model, following steps take place in the kinetics mechanism [17] (adsorption of dye onto the catalyst surface): surface reaction, desorption of products from the surface.

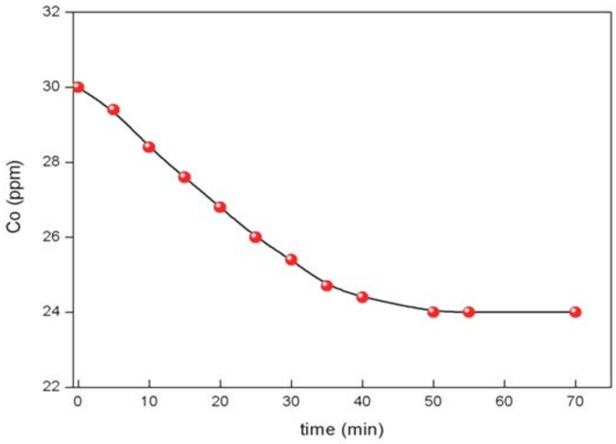

Fig. 3. Determination of the Methyl orange adsorption equilibrium time.

3. Results and discussion

3.1. Influence of the parameters on the degradation of Methyl orange

3.1.1. Effect of initial MO concentration

Fig. 4 shows clearly that the MO degradation is faster for the low concentrations, below 10 mg/L up to 20 mg/L; beyond this concentration, the degradation kinetics is greatly reduced. The latter has been generally interpreted in terms of the increasing screen effect of the pollutant making the photons unavailable for TiO_2 or by a strong adsorption of the dye which then covers a large part of the active sites and reduces the rate of formation of hydroxide radicals.

The photo degradation can occur by one or more active species whose overall mechanism on TiO_2 is as follows:

$$TiO_2 + h\nu \rightarrow h^+_{BV} + e^-_{BC} \text{ (CB: Conduction band)} \qquad (E)$$

$$O_{2ads} + e^-_{BC} \rightarrow O_2^{\bullet -} \qquad (F)$$

$$2O_2^{\bullet -} + 2H_2O \rightarrow H_2O_2 + 2OH^- + O_2 \qquad (G)$$

$$O_{2ads} + e^-_{BC} + H^+ \rightarrow H_2O_2 \qquad (H)$$

$$2H_2O_{2ads} + e^-_{BC} \rightarrow OH^- + {}^\bullet OH \qquad (I)$$

$$H_2O_{ads} + h^+_{BV} \rightarrow {}^\bullet OH + H^+ \text{ (VB: Valence band)} \qquad (J)$$

$${}^\bullet OH_{ads} + h^+_{BV} \rightarrow {}^\bullet OH \qquad (K)$$

$$\text{Pollutant} + ({}^\bullet OH, O_2^{\bullet -}, h^+) \rightarrow \text{by-products} \rightarrow CO_2 + H_2O + \text{mineral salts} \qquad (L)$$

The efficiency of the photocatalytic reaction generally decreases with increasing the initial concentration C_0. High concentrations C_0 lead to an increasing number of MO molecules adsorbed on the surface, thus reducing penetration of photons; which decreases the photo degradation

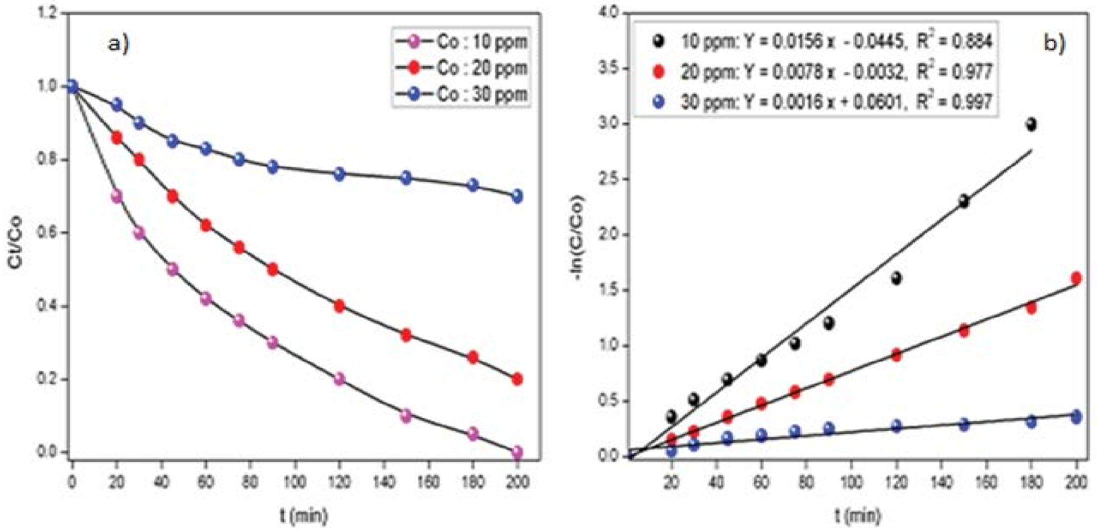

Fig. 4. (a) Methyl orange kinetics of degradation at different initial concentrations in the presence of TiO_2 (1 g/L). (b) Modeling of the degradation kinetics of methyl orange according to the Langmuir–Hinshelwood model.

efficiency (Table 2). According to numerous works [18,19], the photocatalytic degradation rate of most organic compounds is described by the pseudo-first-order kinetics. The pollutant degradation by heterogeneous photocatalysis follows rather the L-H model [20,21], where the oxidation rate is proportional to the fraction of the catalyst surface covered by the MO molecules; the L-H model is given by the following equation:

$$r = \frac{-dC}{dt} = \frac{k_r \cdot K \cdot C}{1 - K \cdot C} \tag{1}$$

For low concentrations ($C < 10^{-3}$ M), the term $K \cdot C$ is negligible in front of 1. Therefore, the reaction follows pseudo-first-order kinetics [22] and Eq. (1) becomes:

$$r = \frac{-dC}{dt} = k_r \cdot K \cdot C = K_{\text{app}} \cdot C \tag{2}$$

whose integration of Eq. (2) gives:

$$\ln \frac{C_0}{C} = K_{\text{app}} \cdot t \tag{3}$$

The initial rate (r_0) is given by:

$$r_0 = \frac{k_r \cdot K \cdot C}{1 + K \cdot C} = K_{\text{app}} \cdot C_0 \tag{4}$$

The half-life time ($t_{1/2}$) is calculated from the following equation:

$$t_{1/2} = \frac{\ln 2}{K_{\text{app}}} \tag{5}$$

where r: photo degradation rate (mg/L min); r_0: initial photo degradation rate (mg/L min); C: the MO concentration at time t (mg/L); k_r: constant of the adsorption equilibrium (mg/L min); K: kinetic constant of L-H (L/mg); $K_{\text{app}} = k_r \cdot K$ apparent rate constant (min⁻¹), that is affected by the concentration C_0.

Table 2
Degradation efficiencies obtained for the different concentrations

C (mg/L)	10	20	30
K_{app} (min^{-1})	0.0156	0.0078	0.0016
R^2	0.884	0.977	0.997
R (%) at $t_{1/2}$	74	53	23
Vo (mg/L min)	0.154	0.156	0.048

The plot $\ln(C_0/C)$ vs. t for different MO concentrations C_0 and various catalyst amounts are illustrated in Fig. 4b. The photocatalytic degradation follows perfectly the pseudo-first-order kinetic for the concentrations C_0 of 10 and 30 mg/L, the constants K_{app} and catalyst amounts are reported in Table 2. The Fig. 4b indicates that the discoloration rate increases with increasing C_0, which corresponds to L-H adsorption model. A linear expression can be occasionally obtained from Eq. (5) by plotting $1/K_{\text{app}}$ against C_0 according to relationship (Eq. (6)) [23]:

$$\frac{1}{K_{\text{app}}} = \frac{1}{k_r} \cdot C_0 + \frac{1}{k_r \cdot K} \tag{6}$$

The constants k_r (0.048 mg L/min) and K (6.246 L/mg) for the MO photocatalytic degradation are determined from the slope ($1/K_{\text{app}}$) and the intercept ($1/k_r \cdot K$).

3.1.2. *Effect of the dose of the TiO_2 catalyst*

The effect of the quantity of TiO_2 on the MO photo degradation was carried out for an initial concentration of 15 mg/L and TiO_2 dose ranging from 0.5 and 1.5 g/L. The degradation kinetics is rapid with the increase in the dose up to 1 g/L, above which only a little improvement is noted (Fig. 5). This threshold is attributed to the total absorption of photons by TiO_2 particles, which are closest to the light source, the increase in the dose from 1 to 2 g/L accompanied by an increase in the number of adsorption sites, and in this way an augmentation of the degradation rate of MO. The absorption rate progresses slightly with the TiO_2 dose; this can be explained on the one hand by the decreased pH of the medium when the TiO_2 amount is increased. This, therefore, modifies the state of the TiO_2 surface and alters significantly the adsorption process. On the other hand, increasing the TiO_2 dose favors the aggregation of particles, which reduces the number of active sites. According to Parida et al. [24], the optimal dose of TiO_2 is 1 g/L for MO concentration of 150 mg/L and an irradiation time of 4 h, the constants of the kinetic model for the different doses of the catalyst are grouped in Table 3.

3.1.3. Effect of pH on the degradation of the MO dye

The pH effect on the photocatalytic elimination of MO (15 mg/L) by TiO_2 (1 g/L) was examined in three pH media: 2.5, 6.5 and 10 (Fig. 6). The obtained results show that at pH 2.5, the degradation of MO is faster; this result can be explained by the attraction forces between the dye and the surface charge of TiO_2, which increases the probability of encountering with the photocatalyst. Conversely, at basic pH, a drop in the photoactivity is observed due to repulsive interactions between the MO species and the surface charge, thus reducing the probability of encountering the photocatalyst.

3.2. Influence of the addition of NaCl and H_2O_2 on the degradation of MO

Fig. 7 shows that the presence of NaCl inhibits the kinetics of the MO photo degradation. The inhibitory effect increases slightly with augmenting the NaCl concentration. This may be due to the adsorption on the active sites of the photocatalyst and/or to its competition with the dye to react with the radicals generated, Cl^- ions can also trap the radical oxidative species.

$$Ox^{\bullet} + Cl \longrightarrow Cl^{\bullet} + Ox^{-} \tag{M}$$

By contrast, the addition of H_2O_2 accelerates the MO degradation, and this can be explained by good sensor of electrons of H_2O_2, which allow it to react with the electrons through a conduction band process according to the following reaction:

$$H_2O_2 + e^-_{BC} \longrightarrow OH^- + {}^{\bullet}OH \tag{N}$$

However, for large H_2O_2 concentrations, the following reaction occurs:

$$H_2O_2 + {}^{\bullet}OH \longrightarrow H_2O + HO_2^{\bullet} \tag{O}$$

Such reaction exerts a negative effect on the kinetics of the photo degradation. Indeed, this reaction consumes the hydroxyl radicals (${}^{\bullet}OH$) normally intended for the MO photo degradation.

3.3. Influence of light flux

Experiments have shown that above a threshold photon flux, the reaction rate decreases the reaction order from 1 to 0.5. Such decrease may be associated with the

Table 3
Determination of degradation coefficients at different TiO_2 doses

Dose g/L	0.5	1.0	2.0
R (%) (t = 60 min)	23	48	59
R (%) (t = 200 min)	70	74	98
R^2	0.978	0.999	0.993
K_{app} (min^{-1})	0.006	0.015	0.024
Vo (g/L min)	0.003	0.015	0.036

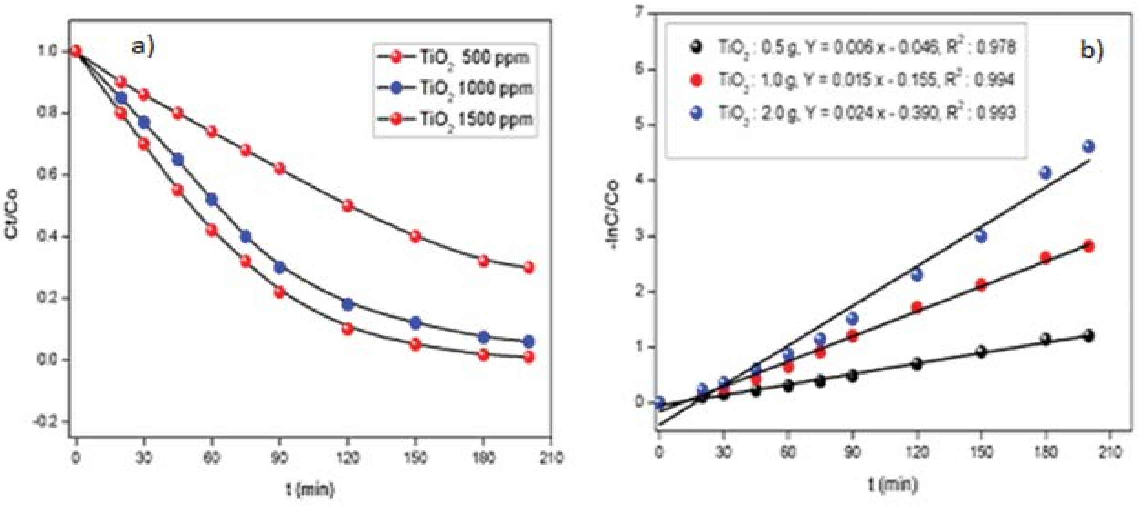

Fig. 5. Methyl orange degradation kinetics for different TiO_2 concentrations.

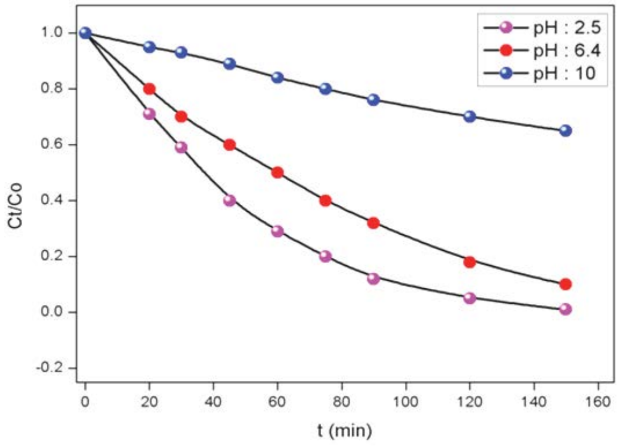

Fig. 6. Influence of pH on the degradation kinetics of methyl orange in presence of TiO_2 (1 g/L).

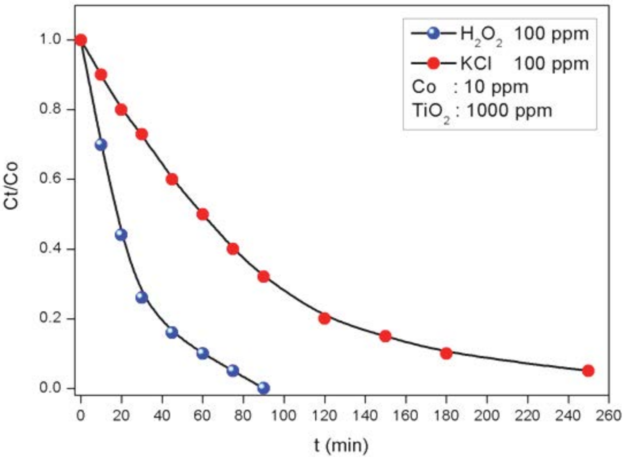

Fig. 7. Influence of H_2O_2 and NaCl on the degradation kinetics of methyl orange in the presence of TiO_2 (1 g/L).

formation of an excess of photogenerated species (e^-, h^+ and $^{\bullet}OH$). On the other hand, for too large light fluxes, we even obtain a zero-order kinetics, indicating that the photocatalytic reaction is no longer dependent on the incident radiation, but mainly on the mass transfer.

4. Conclusion

TiO_2 was used as photocatalyst for the detoxification of water containing methyl orange as a model pollutant. The MO degradation is not directly related to the solar radiation intensity and curiously, high degradation rate needs a limited number of photon.

In order to carry out the photo degradation tests of methyl orange in the presence of TiO_2, first we carried out adsorption tests to determine the equilibrium time which was is 50 min.

The effect of some physical parameters on the kinetics of MO degradation has been studied; the results showed that TiO_2 dose of 0.5 g/L, pH: 2.5, a time of 180 min and MO concentration of 10 ppm gave a better performance, the experimental results obey the L-H model.

The addition of NaCl has no effect on the kinetics while the addition of H_2O_2 increases the degradation yield. The results indicated that the TiO_2 catalyst has a better performance for the water pollution control.

The photocatalysis is an effective method for the dye degradation, on the system TiO_2/UV. It is focused on the generation of (e^-/h^+) pairs; both the charge carriers migrate to the catalyst surface in the presence of the adsorbed azo dyes, where the redox reactions take place. The oxidizing radicals attack the azo dye and convert them partially into CO_2, H_2O and inorganic molecules.

Acknowledgments

The authors gratefully acknowledge the support from the Laboratory of Soft Technologies and Biodiversity, Faculty of Sciences University M'hamed Bougara (Boumerdes). This research did not receive any specific grant from funding agencies in the public, commercial, or not-for-profit sectors.

Conflict of interests

The author(s) declared no potential conflicts of interest with respect to the research, authorship, and/or publication of this article.

References

[1] M.S. Niasari, N. Mir, F. Davar, A novel precursor in preparation and characterization of nickel oxide nanoparticles via thermal decomposition approach, J. Alloys Compd., 493 (2010) 163–168.
[2] M. Abbas, M. Trari, Photocatalytic degradation of Asucryl Red (GRL) in aqueous medium on heat-treated TiO_2 powder - effect of analytical parameters and kinetic modeling, Desal. Water Treat., 180 (2020) 398–404.
[3] S.G. Kumar, L.G. Devi, Review on modified TiO_2 photocatalysis under UV/Visible light: selected results and related mechanisms on interfacial charge carrier transfer dynamics, J. Phys. Chem. A, 115 (2011) 13211–13241.
[4] H. Jia, Z. Zheng, H. Zhao, L. Zhang, Z. Zou, Non aqueous sol–gel synthesis and growth mechanism of single crystalline TiO_2 nanorods with high photocatalytic activity, Mater. Res. Bull., 44 (2009) 1312–1316.
[5] M. Abbas, M. Trari, Contribution of adsorption and photo catalysis for the elimination of Black Eriochrome (NET) in an aqueous medium-optimization of the parameters and kinetics modeling, Sci. Afr., 8 (2020) e 00387.
[6] A.G. Epling, C. Lin, Photoassisted bleaching of dyes utilizing TiO_2 and visible light, Chemosphere, 46 (2002) 561–570.
[7] M. Abbas, T. Aksil, M. Trari, Removal of toxic methyl green (MG) in aqueous solutions by apricot stone activated carbon - equilibrium and isotherms modeling, Desal. Water Treat., V125 (2018) 93–101.
[8] Z. Harrache, M. Abbas, T. Aksil, M. Trari, Modeling of adsorption isotherms of (5, 5′-disodium indigo sulfonate) from aqueous solution onto activated carbon: equilibrium, thermodynamic studies, and error analysis, Desal. Water Treat., 147 (2019) 273–283.
[9] M. Abbas, M. Trari, Removal of Methylene Blue (MB) in Aqueous Solution by Economic Adsorbent Derived from Apricot Stone Activated Carbon (ASAC), Fibers Polym., 21 (2020) 810–820.
[10] M. Abbas, Experimental investigation of activated carbon prepared from apricot stones material (ASM) adsorbent for

removal of malachite green (MG) from aqueous solution, Adsorpt. Sci. Technol., 38 (2020) 24–45.

[11] M. Abbas, Z. Harrache, M. Trari, Mass-transfer processes in the adsorption of crystal violet by activated carbon derived from pomegranate peels: kinetics and thermodynamic studies, J. Eng. Fibers Fabrics, 15 (2020) 1– 11.

[12] M. Abbas, Z. Harrache, M. Trari, Removal of gentian violet in aqueous solution by activated carbon equilibrium, kinetics, and thermodynamic study, Adsorpt. Sci. Technol., 37 (2019) 566–589.

[13] Y. Gao, J.S. Fu, J.B. Drake, J.-F. Lamarque, Y. Liu**,** The impact of emission and climate change on ozone in the United States under representative concentration pathways (RCPs), Atmos. Chem. Phys., 13 (2013) 9607–9621.

[14] Y.L. Cheah, M.A. Simpson, J.J. Pomposelli, E.A. Pomfret, Incidence of death and potentially life threatening near-miss events in living donor hepatic lobectomy: a world-wide survey, Liver Transplant., 19 (2013) 499–506.

[15] T. Mahmood, D. Su, A. Naeem, S. Mustafa, M. Waseem, M. Hamayun, Adsorption of arsenate from aqueous solution on binary mixed oxide of iron and silicon, Chem. Eng. J., 192 (2012) 90–98.

[16] T. Aksil, M. Abbas, M. Trari, S. Benamara, Water adsorption on lyophilized *Arbutus unedo* L. fruit powder: determination of thermodynamic parameters, Microchem. J. 145 (2019) 35–41.

[17] L. Gu, J.Y. Wang, R. Qi, X.Y. Wang, P. Xu, X.J. Han, A novel incorporating style of polyaniline/TiO_2 composites as effective visible photocatalysts, J. Mol. Catal. A, 357 (2012) 19–25.

[18] I. Bouzaida, C. Ferronato, J.M. Chovelon, M.E. Rammah, J.M. Herrmann, Photocatalytic degradation of the anthraquinonic dye, Acid Blue (AB25): a kinetic approach, J. Photochem. Photobiol. A, 168 (2004) 23–30.

[19] E. Bizani, K. Fytianos, I. Poulios, V. Tsiridis, Photocatalytic decolorization and degradation of dye solutions and wastewaters in the presence of titanium dioxide, J. Hazard. Mater., 136 (2006) 85–94.

[20] A. Hamza, I.J. John, B. Mukhtar, Enhanced photocatalytic activity of calcined natural sphalerite under visible light irradiation, J. Mater. Res. Technol., 6 (2017) 1-6.

[21] A. Ounnar, L. Favier, A. Bouzaza, F. Bentahar, M. Trari, Kinetic study of spiramycin removal from aqueous solution using heterogeneous photocatalysis, Kinet. Catal., 57 (2016) 200-206.

[22] A. Kerrami, L. Mahtout, F. Bensouici, M. Bououdina, S. Rabhi, E. Sakher, H. Belkacemi, Synergistic effect of Rutile-Anatase Fe-doped TiO_2 as efficient nanocatalyst for the degradation of Azucryl Red, Mater. Res. Express, 6 (2019) 0850f5, https://doi.org/10.1088/2053-1591/ab2677.

[23] B. Gozmena, M. Turabikb, A. Hesenovc, Photocatalytic degradation of Basic Red 46 and Basic Yellow 28 in single and binary mixture by UV/TiO_2/periodate syste, J. Hazard. Mater., 164 (2009) 1487–1495.

[24] K.M. Parida, N. Sahu, N.R. Biswal, B. Naik, A.C. Pradhan, Preparation, characterization, and photocatalytic activity of sulfate-modified titania for degradation of methyl orange under visible light, J. Colloid Interface Sci., 318 (2008) 231–237.